Signals of two universal extra dimensions at the LHC

G. Burdman[*] and O. J. P. Éboli[†]

Instituto de Física, Universidade de São Paulo, São Paulo—São Paulo 05508-090, Brazil

D. Spehler[‡]

Université de Strasbourg, IPHC, 23 rue du Loess, 67037 Strasbourg, France

Extensions of the standard model with universal extra dimensions are interesting both as phenomenological templates as well as model-building fertile ground. For instance, they are one of the prototypes for theories exhibiting compressed spectra, leading to difficult searches at the LHC since the decay products of new states are soft and immersed in a large standard model background. Here we study the phenomenology at the LHC of theories with two universal extra dimensions. We obtain the current bound by using the production of second level excitations of electroweak gauge bosons decaying to a pair of leptons and study the reach of the LHC Run II in this channel. We also introduce a new channel originating in higher dimensional operators and resulting in the single production of a second level quark excitation. Its subsequent decay into a hard jet and lepton pair resonance would allow the identification of a more model-specific process, unlike the more generic vector resonance signal. We show that the sensitivity of this channel to the compactification scale is very similar to the one obtained using the vector resonance.

I. INTRODUCTION

Since the discovery of the Higgs boson [1,2], the CERN Large Hadron Collider (LHC) has been probing a new energy window, enlarging its potential to search for new physics. Although the Higgs boson completes the standard model (SM) into a renormalizable, spontaneously broken gauge theory in agreement with all experimental data [3,4], there are many questions that remained unanswered. Chief among them is the hierarchy problem, which would require new physics at the TeV scale. Moreover, up to now no definitive signal of new physics has been observed, suggesting that either the new physics is heavy or it is hidden by some mechanism, such as the existence of a compressed spectrum or SM partners without SM quantum numbers.

Extensions of the SM that address the hierarchy problem typically explain the Higgs mass by one of two mechanisms: either supersymmetry is present not far from the weak scale or the Higgs boson is protected by a spontaneously broken global symmetry under which it is a pseudo-Nambu-Goldstone boson. In both cases it is becoming increasingly necessary to explain the absence of signals at hadron colliders, particularly Run I at the LHC. For instance, in supersymmetric theories it is possible to imagine that the spectrum of new particles is dominated by states only coupled to the third generation [5] or that it is too compressed to result in large enough transverse

momenta or missing E_T [6]. It is also possible to build models where the partners of the top quark are not charged under the SM color [7,8], making their observation more difficult at hadron colliders.

An alternative way to introduce new physics at the TeV scale is to assume the existence of compact extra dimensions [9–11]. Universal propagation of all SM fields in the extra dimensions, when supplemented with orbifold boundary conditions, gives the SM as the zero-mode spectrum [12]. At a minimum, the new physics comes in the Kaluza-Klein (KK) tower of excitations. Although generically, extradimensional theories do not solve the (little) hierarchy problem by just lowering the cutoff, it is possible to think that they represent a new strongly coupled sector at the TeV scale. Theories with one extra dimension compactified on an orbifold (S_1/Z_2) have been thoroughly studied [13–18]. When KK parity is assumed to be respected by the boundaries, the resulting spectrum includes a dark matter candidate [19]. Their collider phenomenology is then similar to that of supersymmetric extensions of the SM [13], with cascades typically resulting in large missing transverse momentum. The second KK excitation in these five-dimensional (5D) theories has a mass very close to twice the mass of the first excitation. Thus, production of this level-2 excitation will likely result in decays to two level-1 states, leading to a signal that is difficult to identify at hadron colliders.

Theories with two universal extra dimensions (UED) can be similarly constructed and their phenomenology has been studied already in the literature in various scenarios [20–23] and, in particular, in the context of UED in [24,25]. Just as for 5D UED theories, the level-1 cascade decays give soft

[*]burdman@if.usp.br
[†]eboli@fma.if.usp.br
[‡]spehler@iphc.cnrs.fr

jets and leptons and missing transverse momentum [26]. On the other hand, there are some important differences. From the outset, we notice that level-2 KK excitations have masses that are $\sqrt{2}$ times the level-1 ones. Then, level-2 states cannot decay via the tree level couplings that preserve KK number, but decay through one-loop generated, KK parity preserving couplings [26,27] to SM particles, leading to more identifiable signals at the LHC.

In the present paper we consider the six-dimensional standard model (6DSM) [27] as an example of a model that possesses a compressed spectrum. KK number conservation implies that level-1 KK modes can only be produced in pairs. Their decays contain soft leptons, jets and missing energy making their discovery very difficult [13,26]. On the other hand, level-2 KK states can be singly produced in the s channel [27] and can decay into pairs of SM particles due to KK-number violating interactions.

We examine the LHC potential for studying the 6DSM through the inclusive search for new narrow vector resonances decaying into lepton pairs ($e^{\pm}$ or $\mu^{\pm}$) that takes place via its s-channel production

$$pp \rightarrow W_{\mu}^{3(1,1)}/B_{\mu}^{(1,1)} + X \rightarrow \ell^+ \ell^- + X, \qquad (1)$$

as well as through the resonant production of (1,1) KK quarks in the channel

$$pp \rightarrow Q^{(1,1)} \rightarrow \ell^+ \ell^- + \text{jet}, \qquad (2)$$

where $Q^{(1,1)}$ stands for the (1,1) KK quarks and $W_{\mu}^{3(1,1)}$ and $B_{\mu}^{(1,1)}$ are the level-2 vector states of the SM electroweak gauge bosons.

We show that the level-2 excitations of the electroweak gauge bosons in Eq. (1) provide the best bound for the compactification scale R from available Run I and II data. We then study the reach of the LHC in Run II. For this purpose, we first use the s-channel resonance going into lepton pairs of Eq. (1), but we also add a previously unexplored channel: the single production of a (1,1) quark as in Eq. (2). Although we see that the LHC reach in $1/R$ is similar in this second channel as it is in the dilepton case, this addition constitutes a more model-specific signal since it comes from KK-number violating higher dimensional operators typically present in extradimensional theories, whereas the channel in Eq. (1) is omnipresent in SM extensions. The level-2 quark decays into one of the dilepton resonances and a hard jet, allowing for its reconstruction. Both signals combined would provide an interesting pattern pointing in the direction of further searches and model building based on this simple 6DSM construction.

The rest of the paper is organized as follows: in Sec. II we review the 6DSM, focusing on the main phenomenological facts such as the spectrum and couplings, resulting in specific decay patterns. In Sec. III we obtain the current

bound on $1/R$ using the available LHC Run I and II data. We study the potential of the LHC Run II data in these channels in Sec. IV and conclude in Sec. V.

II. SIX-DIMENSIONAL STANDARD MODEL

We consider the six-dimensional standard model as defined in Ref. [27] where the two extra dimensions form a square $0 \leq x^4, x^5 \leq \pi R$, and are compactified by identifying pairs of adjacent sides, the so-called "chiral square" [24,25]. The extradimensional space is symmetric under reflections with respect of the center of the square, this being the KK parity symmetry that we label Z_2^{KK}.

In order to ensure 6D anomaly cancellation [28], the weak-doublet quarks have the opposite 6D chiralities than the singlet ones, i.e., labeling the 6D chiralities as $\pm$ we have $Q_+ = (U_+, D_+)$, U_-, and D_-. In addition to these states the model contains 6D gauge bosons and leptons. The KK expansion of a six-dimensional field Φ possessing a zero mode can be written as

$$\Phi = \sum_{j,k} \left(\cos \frac{jx^4 + kx^5}{R} + \cos \frac{kx^4 - jx^5}{R} \right) \frac{\Phi^{(j,k)}(x^\mu)}{\pi R(1 + \delta_{j,0})}, \qquad (3)$$

where the KK numbers j and k are integers satisfying $j \geq 1$ and $k \geq 0$ or $j = k = 0$. At tree level, the masses of the four-dimensional (4D) KK modes $\Phi^{(j,k)}$ are

$$M_{j,k} = \sqrt{j^2 + k^2} \frac{1}{R}. \qquad (4)$$

In the 6DSM each 6D gauge boson (V) decomposes into a tower of 4D spin-0 ($V_H^{(j,k)}$) and spin-1 ($V_\mu^{(j,k)}$) fields [24,25]. On the other hand, the 6D lepton and quark fields give rise to a tower of massive vectorlike 4D fermions and a chiral zero mode that we identify with the known fermions.

In addition to the bulk action, the theory admits operators localized at the fixed points of the chiral square, i.e., the points (0,0), $(\pi R, \pi R)$, and $(0, \pi R) \equiv (\pi R, 0)$. These are induced by loops involving the 6D bulk interactions [29], as well as by physics above the cutoff scale. Generically, we have [27]

$$\int_0^{\pi R} dx_4 \int_0^{\pi R} dx_5 \{ \mathcal{L}_{\text{bulk}} + \delta(x_4)\delta(x_5 - \pi R)\mathcal{L}_2 + [\delta(x_4)\delta(x_5) + \delta(x_4 - \pi R)\delta(x_5 - \pi R)]\mathcal{L}_1 \}, \qquad (5)$$

which reflects the identification of the points at $(0, \pi R)$ and $(\pi R, 0)$, as well as the KK parity, Z_2^{KK}, resulting in identical operators at (0,0) and $(\pi R, \pi R)$. Here $\mathcal{L}_{\text{bulk}}$ is the bulk 6D Lagrangian including all the SM field kinetic terms as well as the appropriate Yukawa couplings and Higgs potential needed in order to obtain the SM as the zero-mode spectrum. The terms $\mathcal{L}_1$ and $\mathcal{L}_2$ contain all possible
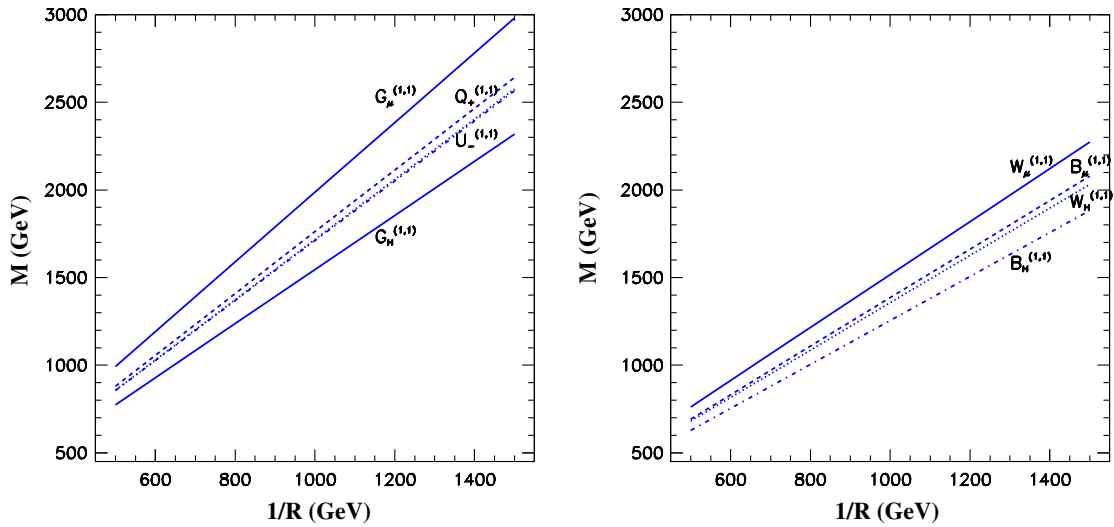
FIG. 1.   Mass spectrum of the (1,1) KK states as a function of $1/R$. In the left panel we depict the masses of the strongly interacting states while the right panel contains the (1,1) KK states associated to the 6D electroweak gauge bosons. Notice that the states $U_-^{(1,1)}$ and $D_-^{(1,1)}$ are almost degenerate.

localized operators consistent with the 4D symmetries of the SM as well as the pieces that correspond to the motion along the two extra dimensions. For instance, the lowest-dimension localized operator involving the 6D U_- quark field is

$$\frac{C_{pU}}{\Lambda^2}(\bar{U}_{-R}i\Gamma_\mu D^\mu U_{-R} + \bar{U}_{-L}i\Gamma_\mu D^\mu U_{-L})$$
$$+ \left(\frac{C'_{pU}}{\Lambda^2}\bar{U}_{-R}i\Gamma_\ell U_{-L} + \text{H.c.}\right), \tag{6}$$

where Γ_μ with $\mu = 0, 1, 2, 3$, and Γ_ℓ with $\ell = 4, 5$ are 8×8 anticommuting matrices defining the Clifford algebra in 6D, D_μ, and D_ℓ are covariant derivatives, and the order one coefficients C_{pU} and C'_{pU} are partly determined by the physics above the cutoff Λ, plus renormalizations arising below it. The index $p = 1, 2$ refers to operators belonging to $\mathcal{L}_1$ and $\mathcal{L}_2$. Similarly, localized operators containing the 6D gluon field give rise to the following lowest mass dimension operators:

$$-\frac{1}{4}\frac{C_{pG}}{\Lambda^2}G_{\mu\nu}G^{\mu\nu} - \frac{1}{2}\frac{C'_{pG}}{\Lambda^2}(G_{45})^2. \tag{7}$$

The presence of these localized operators results in interactions violating KK number conservation but respecting the Z_2^{KK} parity. Additionally, these operators result in corrections to the masses of the KK tower that would depend on the gauge charges of the fields. For illustration, we present in Fig. 1 the expected mass spectrum of the (1,1) KK states where we used the expressions given in Ref. [27,30] and we chose the cutoff scale $\Lambda = 10/R$. The splitting in the spectrum does allow for KK-number

conserving cascade decays of strongly produced KK states into lighter ones, albeit with difficult to observe final states.

More promising signals result from the KK-number violating interactions induced by localized operators such as the ones in Eqs. (6) and (7). The Z_2^{KK} implies that the sum over all j and k numbers must be even in interactions among the KK states. Bulk interactions do not generate interactions between a KK mode and two zero modes since they respect KK number. However, localized operators can give rise to them allowing the decay of a KK state directly into two SM particles [27]. For instance, KK-number violating couplings between a massive KK gluon and SM quarks are described by the operator [27]

$$g_s C_{j,k}^{qG}(\bar{q}\gamma^\nu T^a q)G_\nu^{(j,k)a}, \tag{8}$$

where T^a are the $SU(3)_c$ generators in the fundamental representation. The coefficient $C_{j,k}^{qG}$ receives contributions from the localized operators in Eqs. (6) and (7) through the renormalizations of the quark and gluon lines they induce. There are similar interactions for the electroweak states $W_\mu^{(j,k)a}$ and $B_\mu^{(j,k)}$ with the natural adjustments for a different gauge group.

As shown in Ref. [27] the existence of these KK-number violating interactions such as in Eq. (8) has important consequences for the search of (1,1) KK states of the gauge bosons. Since their masses are $\sqrt{2}$ times the (1,0) masses, they cannot decay into them. Then, although the couplings in Eq. (8) are volume suppressed when compared with the KK-conserving ones, they determine the (1,1) decay channels.

In addition, here we show that there are operators of higher mass dimensions that are potentially as important as these in the phenomenology at the LHC. In particular, we
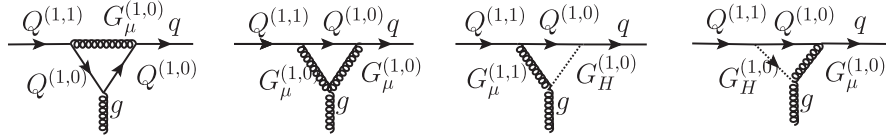
FIG. 2. Feynman diagrams contributing to the one-loop process $Q^{(1,1)} \to qg$.

study localized operators that allow the direct coupling of (1,1) KK quarks to pairs of SM particles. Of interest to us here is the one-loop induced process

$$qg \to Q^{(1,1)}, \tag{9}$$

where Q stands for any of the (1,1) KK states of the quarks while q (g) represents a SM light quark (gluon).

In order to generate a process like Eq. (9) via localized operators we need to go to operators of higher mass dimensions than the ones leading to Eq. (8). The reason is that to obtain nondiagonal (in KK number) gluon couplings to quark fields, these cannot come from kinetic-like localized operators since these interactions are always diagonal due to gauge invariance. On the other hand, higher dimensional localized operators such as

$$\mathcal{O}_1 = \bar{U}\Gamma^\mu D^\nu U G_{\mu\nu} \quad \text{and} \quad \mathcal{O}_2 = \bar{U}\sigma^{\mu\nu} U G_{\mu\nu} \tag{10}$$

lead to processes like Eq. (9).

Expanding the 6D fields in Eq. (10) into KK modes results in the effective Lagrangian for the process of interest given by

$$f_1 \overline{Q^{(1,1)}} \gamma^\mu D^\nu T^a q G^a_{\mu\nu} + f_2 \overline{Q^{(1,1)}} \sigma^{\mu\nu} T^a q G^a_{\mu\nu} \tag{11}$$

where $f_{1,2}$ are functions of the momenta of the particles and R. Notice that the effective operators in Eq. (11) allow the single production of (1,1) KK quarks that has the potential of enlarging the LHC capabilities to search for these particles as we show below.

We can estimate the coefficients of the operators in Eq. (10) by computing the one-loop contributions to them coming from KK excitations through bulk vertices that respect KK number. In Fig. 2 we show the Feynman diagrams corresponding to these one-loop contributions, which are finite. The Wilson coefficients of the operators given by Eq. (11) are given by

$$f_1 = \frac{\alpha_s^{3/2}}{\sqrt{4\pi}} \{ (C_2(R) - C_2(G))(8C_{23} - 4C_{22} - 4C_{21})$$
$$+ 2C_2(R)C_0 + C_2(G)(-C_0 + C_{12} - C_{11}) \},$$

$$f_2 = \frac{\alpha_s^{3/2}}{\sqrt{4\pi}} \{ 4(C_2(R) - C_2(G))(C_{23} - C_{21}) + 2C_2(R)C_0$$
$$+ (-3C_0 - 3C_{12} + C_{11}) \}, \tag{12}$$

where the C_X are the Passarino-Veltman functions [31] evaluated at $C_x(0, 0, M_{11}^2, M_{10}^2, M_{10}^2)$, with the M_{ij} being the masses of the (i, j) KK state, and $C_2(R) = 4/3$ and $C_2(G) = 3$ are the Casimir invariants of the fundamental and adjoint representations of $SU(3)$, respectively. Although the coefficient functions f_1 and f_2 generally receive additional contributions from the UV, we estimate their size by the one-loop contributions from Fig. 2 and detailed in Eq. (12).

In what follows we study the phenomenology of the (1,1) KK modes. Although the bulk KK-number conserving interactions mediate the decay of a given (1,1) state into a lighter (1,1) state plus a SM particle, localized KK-number violating interactions open up decays of (1,1) states to a pair of SM particles [27]. These are often the preferred modes, as can be seen in Table I, where the $B_\mu^{(1,1)}$ and $W_\mu^{3(1,1)}$ branching ratios are clearly dominated by KK-number violating interactions. Moreover, the KK-number violating interactions are also responsible for the decays of the spin-0 adjoint states $G_H^{(1,1)}$, $W_H^{3(1,1)}$, and $B_H^{(1,1)}$ into top-quark pairs since their couplings to fermions are proportional to the fermion mass [24].

On the other hand the decay of the (1,1) KK quarks takes place mostly through KK-conserving interactions as can be seen in Table II. In fact, we verified that the branching ratio of the (1,1) KK quarks into quark-gluon pairs via the interactions in Eq. (11) is negligible. Thus, we can make use of the single production of the (1,1) quark through Eq. (9) followed by its decays into $W_\mu^{(1,1)}$ plus jet and $B_\mu^{(1,1)}$ plus jet. This provides an additional search channel for a 6DSM signal: s-channel resonant production of (1,1) KK quarks.

Taking into account that the branching ratios shown in Tables I and II for $1/R = 1$ TeV do not change much when we vary R, we see that inclusive channels containing

TABLE I. Two-body decays of $B_\mu^{(1,1)}$ and $W_\mu^{3(1,1)}$ and respective branching ratios for $1/R = 1$ TeV.

Decay mode	$B_\mu^{(1,1)}$	$W_\mu^{3(1,1)}$
$t\bar{t}$	29%	15%
$b\bar{b}$	7%	16%
Light dijet	60%	50%
$\sum \ell^+ \ell^-$	3%	0.05%
$\sum \nu\bar{\nu}$	1%	0.05%
$\sum L^{(1,1)} + \ell$	$\cdots$	19%

TABLE II. Branching ratios of (1,1) KK quarks of the first two generations for $1/R = 1$ TeV.

Decay mode	$Q_+^{(1,1)}$	$U_-^{(1,1)}$	$D_-^{(1,1)}$
$G_H^{(1,1)}q$	42%	64%	87%
$W_H^{3(1,1)}q$	24%	…	…
$\sum_j W_\mu^{j(1,1)}q$	32%	…	…
$B_H^{(1,1)}q$	0.4%	12%	4%
$B_\mu^{(1,1)}q$	0.8%	24%	9%

leptons lead to the first signal of the existence of the 6DSM. This is the case despite the fact that the main decay modes of the (1,1) KK quarks are into the scalar adjoints $G_H^{(1,1)}$, $W_H^{3(1,1)}$, $B_H^{(1,1)}$ followed by their decays into top pairs. Actually, if a signal is observed in the lepton channels, then the decays of the (1,1) KK quarks into scalar adjoints resulting in a $t\bar{t} + j$ signal can be used to decide if the resonance corresponding to the dilepton + jet is consistent with the 6DSM or the 5D case. This is because in the 5D case there are no scalar adjoints [27] (which decay overwhelmingly to top pairs) in the spectrum and the decay channels of the level-2 KK quarks are into level-2 electroweak gauge bosons plus a jet [13]. These lead to final states that are more evenly distributed among dijets, $b\bar{b}$, $t\bar{t}$ and dileptons plus a hard jet. The dominance of the scalar adjoint channels provides this discrimination only once enough luminosity is accumulated, since the $t\bar{t} + j$ resonance search is afflicted by larger backgrounds than the dilepton $+j$ case.

In the next section we obtain bounds on $1/R$ using the lepton channels with the available LHC Run I and II data at $\sqrt{s} = 8$ and 13 TeV, respectively. We then make sensitivity predictions for the LHC at $\sqrt{s} = 13$ TeV in this channel for larger integrated luminosities. But in addition, we also make use of the singly produced (1,1) KK quark with its subsequent KK-number conserving decays to a charged lepton pair and a hard jet to show that this is a complementary channel that can prove important in pinning down the origin of the signals being observed beyond the rather ubiquitous vector resonance signal.

III. PRESENT BOUNDS ON THE 6DSM

We start by making use of the LHC Runs I and II available data in order to extract the current bound on $1/R$ in the 6DSM. In particular, the CMS collaboration searched for narrow resonances (V) decaying into e^+e^- or $\mu^+\mu^-$ pairs at the center-of-mass energies of 8 and 13 TeV and integrated luminosities of 20.6 and 2.6 fb^{-1}, respectively [32,33]. The analysis was based on the ratio between inclusive production cross sections

$$R_\sigma = \frac{\sigma(pp \to V + X \to \ell^+\ell^- + X)}{\sigma(pp \to Z + X \to \ell^+\ell^- + X)}, \qquad (13)$$

where $\ell = e$ or μ and the V production cross section was obtained using a window of 40% of its mass in the 8 TeV analysis and the narrow width approximation in the 13 TeV one. On the other hand, the Z production cross section used a mass window of ± 30 GeV in both analyses. The 6DSM contribution to R_σ originates from the processes in Eqs. (1) and (2).

In our analysis we evaluated the relevant cross sections at tree level using the package MADGRAPH [34] where the 6DSM was inputed using FeynRules [35]. In Fig. 3 we
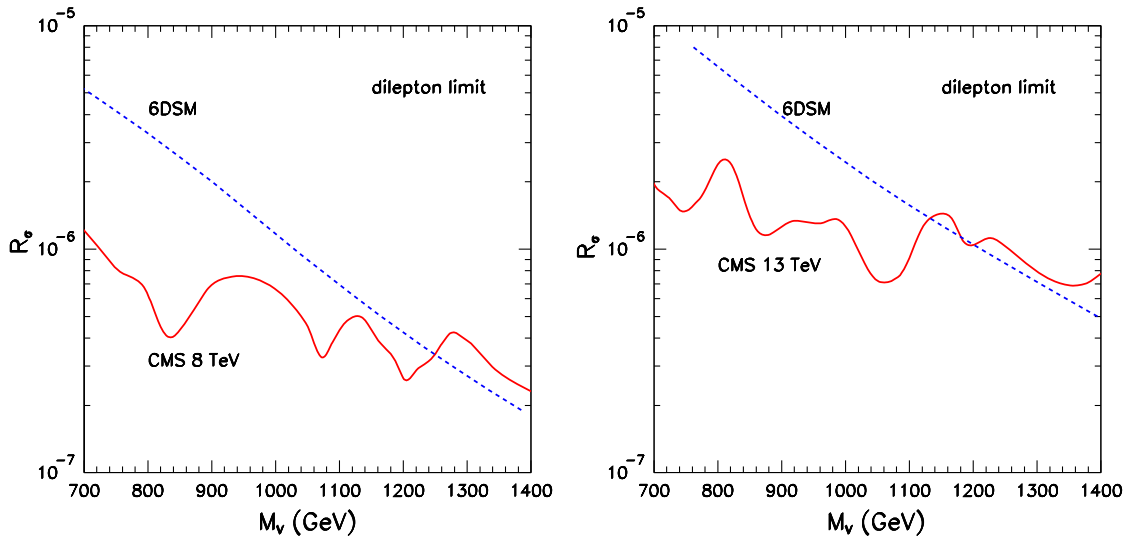

FIG. 3. The solid red line stands for the CMS 95% C.L. upper limit on the ratio R_σ of a narrow resonance decaying e^+e^- and $\mu^+\mu^-$ pairs as a function of the resonance mass M_V in GeV. The dashed blue line represents the six-dimensional standard model prediction for R_σ. The left (right) panel contains the 8 (13) TeV results.

show the present CMS 8 and 13 TeV limits on R_σ as a function of the mass of the new narrow resonance, as well as the 6DSM prediction. The 6DSM cross section is dominated by the $B_\mu^{(1,1)}$ production with a few percent contribution from $W_\mu^{3(1,1)}$; see Table I. As we can see from the left panel of this figure, the CMS Run I data lead to the 95% C.L. constraint

$$M_V > 1250 \text{ GeV} \qquad (14)$$

that can be translated into

$$\frac{1}{R} > 900 \text{ GeV}. \qquad (15)$$

On the other hand the limits originating from the 13 TeV data, i.e., $M_V > 1140 \text{ GeV}$ and $1/R > 820 \text{ GeV}$, are weaker than the ones coming from Run I, due to the small 13 TeV integrated luminosity. Furthermore, it is interesting to notice that the above limit on $1/R$ is very close to the indirect bound that can be obtained from the precision electroweak measurements that lead to $1/R > 920 \text{ GeV}$ at 95% C.L. [36].

Other potentially interesting bounds can come from the spinless adjoints $G_H^{(1,1)}$, $W_H^{3(1,1)}$, and $B_H^{(1,1)}$, which appear in the spectrum of the 6DSM given that only one combination of Nambu-Goldstone bosons is eaten by the KK excitations. Since they couple to mass they decay predominantly into top-quark pairs [27]. The ATLAS and CMS collaborations looked for $t\bar{t}$ resonances at the LHC with a center-of-mass energy of 8 TeV [37,38]. We verified that the present available limits on the production cross section of $t\bar{t}$ resonances do not lead to competitive bounds on the 6DSM.

IV. LHC POTENTIAL TO FURTHER PROBE THE 6DSM

In evaluating the LHC reach for finding the 6DSM we consider two strategies. The first is the search for opposite charge dilepton $\ell^+\ell^-$ resonances with $\ell^\pm = e^\pm$ or $\mu^\pm$. The dilepton pairs originated from the s-channel production of $B_\mu^{(1,1)}$ and $W_\mu^{3(1,1)}$, as well as from the (1,1) KK quark decays into these (1,1) vector resonances, followed by their decays to lepton pairs with the branching ratios detailed in Table I. Although these branching fractions are small, the cleanliness of the signal allows for interesting bounds, as we saw in the previous section for the Runs I and II results. On the other hand, a dilepton resonance is present in many extensions of the SM and it would be good to have a signal that is more model specific. Thus, our second strategy is to look for the single production of a (1,1) excited quark and its subsequent decay into a jet and a lepton pair resonance, either $B_\mu^{(1,1)}$ or $W_\mu^{3(1,1)}$. The single (1,1) quark production mechanism coming from higher dimensional operators is a

sign that we would be in the presence of nonrenormalizable interactions suppressed by not such a high scale, a typical feature of the 6DSM. In what follows we detail these two strategies and their reach in Run II at the LHC.

A. Search for new resonances in the inclusive $\ell^+\ell^-$ final state

The 6DSM contributes to the inclusive production of dilepton resonances through the production of the (1,1) KK vector bosons $B_\mu^{(1,1)}$ and $W_\mu^{3(1,1)}$ by the processes given in Eqs. (1) and (2). The main SM backgrounds for these are the processes [33]

$$pp \to \ell^+\ell^- + X,$$
$$pp \to W^+W^-/ZZ \to \ell^+\ell^-\nu_\ell\bar{\nu}_\ell,$$
$$pp \to t\bar{t} \to \ell^+\ell^-\nu_\ell\bar{\nu}_\ell + \text{jets}. \qquad (16)$$

Initially we evaluated the LHC potential to constrain the 6DSM via the resonance search in the dilepton channel assuming a center-of-mass energy of 13 TeV and an integrated luminosity of 30(100) fb^{-1}. In this first scenario we assumed that the number of observed events agrees with the SM prediction to extract the attainable 95% C.L. limits on the mass of the vector resonances or on the compactification radius R. Once again we simulated the signal in Eqs. (1) and (2), as well as the SM backgrounds in Eq. (16) at tree level using the package MADGRAPH. We added the $\mu^+\mu^-$ and e^+e^- contributions assuming that the muon reconstruction efficiency is close to 100% and the electron/positron one is 90%.

In our analysis of the inclusive dilepton signal we imposed very simple acceptance cuts on the charged leptons

$$|\eta_\ell| < 2.5 \quad \text{and} \quad p_T > 100 \text{ GeV}. \qquad (17)$$

We also required that the dilepton invariant mass ($m_{\ell\ell}$) lay in a window around the resonance mass M_V whose width is 10% of M_V, i.e.,

$$|m_{\ell\ell} - M_V| < 0.05 \times M_V. \qquad (18)$$

We present in Fig. 4 the limit on new resonance contributions to the inclusive cross section after cuts as a function of M_V (left panel) and reinterpret it as a bound on $1/R$ (right panel) for integrated luminosities of 30 (dotted blue line) and 100 fb^{-1} (dashed red line). As we can see from this figure the LHC with a center-of-mass energy of 13 TeV is able to exclude at 95% C.L. (1,1) vector resonances with masses up to 2.0 (2.4) TeV for 30(100) fb^{-1}. These bounds correspond to limits on $1/R$ of 1.4 (1.7) TeV, respectively.

In order to assess the LHC discovery potential of the six-dimensional standard model through the inclusive dilepton
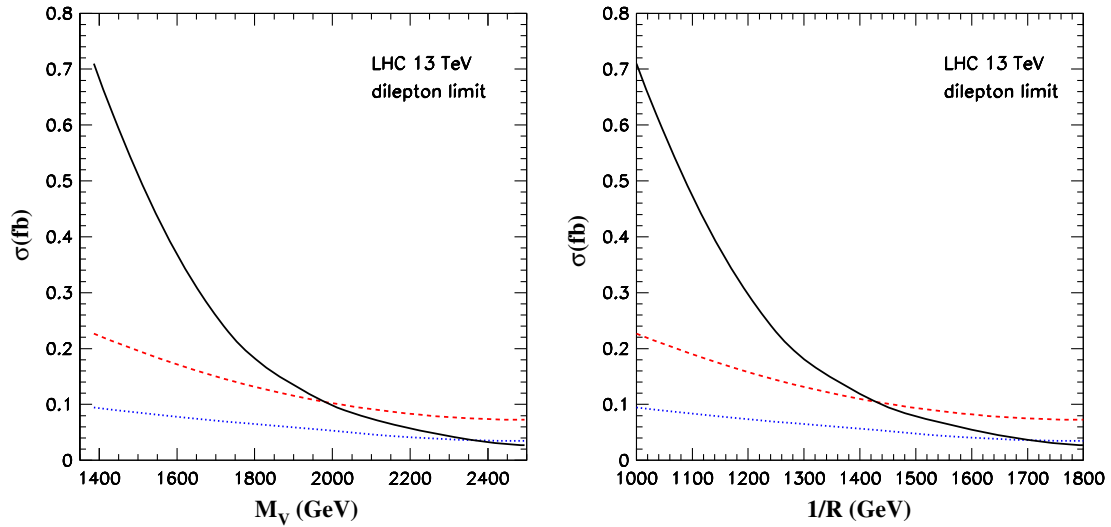
FIG. 4. 95% C.L. attainable limits on new resonance contribution to the dilepton production cross section as a function of the $B_\mu^{(1,1)}$ mass (left) or as a function of $1/R$ (right). The dashed red (dotted blue) curve stands for the limit on the production cross section after cuts assuming an integrated luminosity of 30(100) fb^{-1}. The new contribution to the dilepton production cross section due to the six-dimensional standard model is depicted by the solid black line.

channel we determine the integrated luminosity necessary for a 5σ discovery; our results are shown in Fig. 5. As we can see from the left panel of this figure, the LHC can discover $B_\mu^{(1,1)}$ with masses up to 1530 (1850) GeV for an integrated luminosity of 30(100) fb^{-1}. From the right panel of the same figure, we can see that the LHC can unravel signals of the 6DSM for compactification scales $(1/R)$ 1100 (1340) GeV for the above integrated luminosities, respectively.

B. Search for (1,1) KK quarks

We can also look for the six-dimensional standard model through the single production of (1,1) KK quarks as in

Eq. (2). As mentioned earlier, the added advantage of this mode is that it is more model specific since it requires a specific spectrum tied to a particular structure of higher dimensional operators, making this single production channel possible. Furthermore, the fact that the (1,1) KK quark decays to the dilepton resonance [$W_\mu^{3(1,1)}$ or $B_\mu^{(1,1)}$] plus a hard jet allows the reconstruction of two states of the 6DSM spectrum in one decay channel.

The main standard model backgrounds for this process are the Drell-Yan and W^+W^-/ZZ productions accompanied by a jet as well as top-quark pair production.

In order to extract the signal of KK (1,1) quarks from the background we required two hard charged leptons (e^+e^- or
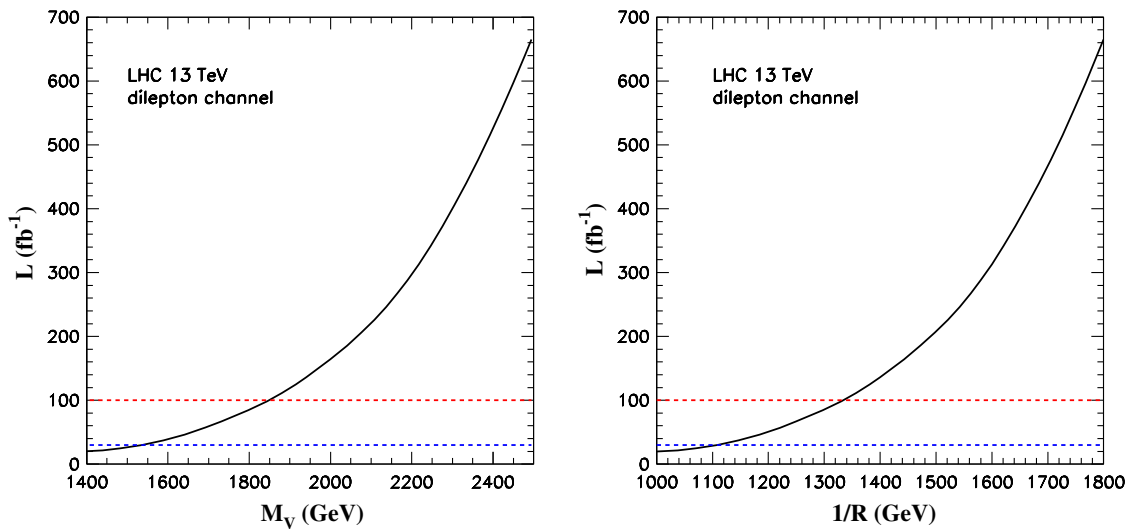

FIG. 5. Integrated luminosity required for a 5σ discovery of the six-dimension standard model (solid black curve) as a function of $B_\mu^{(1,1)}$ mass (left panel) and $1/R$ (right panel). Just for reference we show the lines for 30 and 100 fb^{-1}.
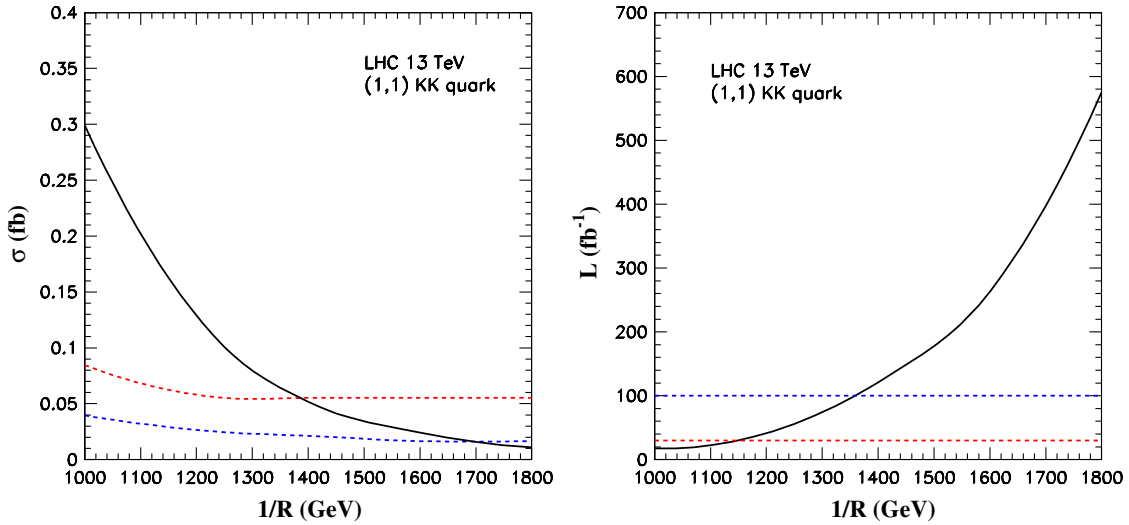
FIG. 6. Left panel: 95% C.L. attainable limits on production cross section of (1,1) KK quarks as a function of $1/R$. In this panel, the blue (red) dashed curve stands for the limit on the production cross section after cuts assuming an integrated luminosity of 30(100) fb^{-1}, while the solid black line stands for the expected production cross section within the six-dimensional standard model framework. Right panel: Integrated luminosity required for a 5σ discovery of (1,1) KK quarks (red curve) as a function of $1/R$. Just for reference we show the lines for 30 and 100 fb^{-1}.

$\mu^+\mu^-$) as in Eq. (17), as well as the presence of an energetic jet in the event satisfying

$$|\eta_j| < 5 \quad \text{and} \quad p_T^j > 200 \text{ GeV}. \quad (19)$$

Since the lepton pair originates from the decay of an on-shell $B_\mu^{(1,1)}$ or $W_\mu^{(1,1)}$ we required the dilepton invariant mass to be large,

$$M_{\ell\ell} > 1.3 \times \frac{1}{R}, \quad (20)$$

where R is the compactification scale being probed. Furthermore, we added the signal for the production of $D_-^{(1,1)}$, $D_+^{(1,1)}$, $U_-^{(1,1)}$, and $U_+^{(1,1)}$ by requiring that the invariant mass of the dilepton pair and the most energetic jet satisfies

$$M_{D_-^{(1,1)}} - 150 < M_{\ell\ell j} < M_{U_+^{(1,1)}} + 150 \text{ GeV}, \quad (21)$$

where the masses are the ones corresponding to the scale $1/R$.

Assuming that just the SM background is observed in the channel given by Eq. (2), we depict in the left panel of Fig. 6 the attainable limits on the (1,1) KK production cross section for integrated luminosities of 30 (blue dashed line) and 100 fb^{-1} (red dashed line) as well as the 6DSM expected cross section (solid black line). As we can see, using this channel the LHC run at 13 TeV has the potential of ruling out compactification scales $(1/R)$ 1.4 and 1.7 TeV for these integrated luminosities, respectively.

The right panel of Fig. 6 displays the integrated luminosity needed to establish a 5σ discovery of a (1,1) KK quark as a function of $1/R$. It is interesting to notice that this channel can establish the 6DSM for compactification scales $(1/R)$ 1140 and 1360 GeV for integrated luminosities of 30 and 100 fb^{-1}, respectively. These values of R correspond to (1,1) KK quark masses around 2 and 2.3 TeV. Moreover, the reach in this channel is slightly larger than the one in the dilepton channel for the same integrated luminosity.

V. CONCLUSIONS

We have examined the present status and future potential of the LHC bounds on two universal extra dimensions. The present limits from the CMS available data we extracted in Sec. III were obtained by simply using the inclusive production of the (1,1) excitations of the electroweak gauge bosons, $W_\mu^{3(1,1)}$ and $B_\mu^{(1,1)}$, and their subsequent decays to lepton pairs. The first excitations (1,0) decay mostly through KK-number conserving interactions resulting in low p_T tracks and missing E_T. The fact that the (1,1) modes are only $\sqrt{2}$ heavier than this so they must decay to SM states through KK-number violating interactions makes these modes easier to search for at the LHC. In fact, the bound extracted from the Run I data in these channels, $1/R > 900$ GeV, is comparable to the indirect bound obtained by using electroweak precision measurements [36].

We have also explored the LHC Run II reach at $\sqrt{s} = 13$ TeV both in the dilepton resonance as well as

in the singly produced (1,1) quarks. Although the sensitivity in $1/R$ is similar in both channels, the (1,1) quark channel has the added advantage of being more model specific when compared to the production of a vector resonance decaying to a pair of leptons. It is also interesting that in this channel it would be possible to reconstruct not only the dilepton resonance, but also the (1,1) quark itself when the dilepton is combined with the very hard jet. A more detailed simulation of this reconstruction is needed, which we leave for future work.

[1] G. Aad *et al.* (ATLAS Collaboration), Phys. Lett. B **716**, 1 (2012).

[2] S. Chatrchyan *et al.* (CMS Collaboration), Phys. Lett. B **716**, 30 (2012).

[3] See K. A. Olive *et al.* (Particle Data Group Collaboration), Chin. Phys. C **38**, 090001 (2014) and references therein.

[4] See T. Corbett, O. J. P. Eboli, D. Goncalves, J. Gonzalez-Fraile, T. Plehn, and M. Rauch, J. High Energy Phys. 08 (2015) 156; A. Butter, O. J. P. boli, J. Gonzalez-Fraile, M. C. Gonzalez-Garcia, T. Plehn, and M. Rauch, J. High Energy Phys. 07 (2016) 152 and references therein.

[5] M. Papucci, J. T. Ruderman, and A. Weiler, J. High Energy Phys. 09 (2012) 035.

[6] S. P. Martin, Phys. Rev. D **75**, 115005 (2007).

[7] G. Burdman, Z. Chacko, H. S. Goh, and R. Harnik, J. High Energy Phys. 02 (2007) 009.

[8] Z. Chacko, H. S. Goh, and R. Harnik, Phys. Rev. Lett. **96**, 231802 (2006).

[9] I. Antoniadis, Phys. Lett. B **246**, 377 (1990).

[10] N. Arkani-Hamed, S. Dimopoulos, and G. R. Dvali, Phys. Lett. B **429**, 263 (1998).

[11] L. Randall and R. Sundrum, Phys. Rev. Lett. **83**, 3370 (1999).

[12] T. Appelquist, H. C. Cheng, and B. A. Dobrescu, Phys. Rev. D **64**, 035002 (2001).

[13] H. C. Cheng, K. T. Matchev, and M. Schmaltz, Phys. Rev. D **66**, 056006 (2002).

[14] L. Edelhuser, T. Flacke, and M. Krmer, J. High Energy Phys. 08 (2013) 091.

[15] G. Cacciapaglia, A. Deandrea, J. Ellis, J. Marrouche, and L. Panizzi, Phys. Rev. D **87**, 075006 (2013).

[16] A. Belyaev, M. Brown, J. Moreno, and C. Papineau, J. High Energy Phys. 06 (2013) 080.

[17] For a recent review, see G. Servant, Mod. Phys. Lett. A **30**, 1540011 (2015).

[18] D. Choudhury and K. Ghosh, arXiv:1606.04084; K. Ghosh, J. High Energy Phys. 04 (2009) 049.

[19] G. Servant and T. M. P. Tait, Nucl. Phys. **B650**, 391 (2003).

[20] P. Fayet, Phys. Lett. B **159B**, 121 (1985).

[21] I. Antoniadis, K. Benakli, and M. Quiros, Phys. Lett. B **331**, 313 (1994).

[22] I. Antoniadis, K. Benakli, and M. Quiros, Phys. Lett. B **460**, 176 (1999).

[23] P. Nath, Y. Yamada, and M. Yamaguchi, Phys. Lett. B **466**, 100 (1999).

[24] G. Burdman, B. A. Dobrescu, and E. Ponton, J. High Energy Phys. 02 (2006) 033.

[25] E. Ponton and L. Wang, J. High Energy Phys. 11 (2006) 018.

[26] D. Choudhury, A. Datta, D. K. Ghosh, and K. Ghosh, J. High Energy Phys. 04 (2012) 057.

[27] G. Burdman, B. A. Dobrescu, and E. Ponton, Phys. Rev. D **74**, 075008 (2006).

[28] B. A. Dobrescu and E. Poppitz, Phys. Rev. Lett. **87**, 031801 (2001).

[29] H. Georgi, A. K. Grant, and G. Hailu, Phys. Lett. B **506**, 207 (2001).

[30] H. C. Cheng, K. T. Matchev, and M. Schmaltz, Phys. Rev. D **66**, 036005 (2002).

[31] G. Passarino and M. J. G. Veltman, Nucl. Phys. **B160**, 151 (1979).

[32] CMS Collaboration, Report No. CMS-PAS-EXO-12-061.

[33] CMS Collaboration, Report No. CMS-PAS-EXO-15-005.

[34] J. Alwall, R. Frederix, S. Frixione, V. Hirschi, F. Maltoni, O. Mattelaer, H.-S. Shao, T. Stelzer, P. Torrielli, and M. Zaro, J. High Energy Phys. 07 (2014) 079.

[35] A. Alloul, N. D. Christensen, C. Degrande, C. Duhr, and B. Fuks, Comput. Phys. Commun. **185**, 2250 (2014).

[36] T. Kakuda, K. Nishiwaki, K. y. Oda, and R. Watanabe, Phys. Rev. D **88**, 035007 (2013).

[37] The ATLAS Collaboration, Report No. ATLAS-CONF-2013-052.

[38] S. Chatrchyan *et al.* (CMS Collaboration), Phys. Rev. Lett. **111**, 211804 (2013); **112**, 119903(E) (2014).